RSC Advances

ROYAL SOCIETY OF CHEMISTRY

www.rsc.org/advances

Lanthanum Strontium Manganese Oxide (LSMO) nanoparticles for anticancer therapy and diagnostics

Vaishnavi M. Kulkarni, Dhananjay Bodas and Kishore M. Paknikar

Center for Nanobioscience, Agharkar Research Institute, G. G. Agarkar road, Pune 411004 India

Telefax: +91-20-25653860 Email: kpaknikar@gmail.com; dsbodas@aripune.org

Keywords:

LSMO nanoparticles, magnetic fluid hyperthermia, radio frequency induced heating, MRI, anti-cancer therapy, drug delivery

Abstract:

Lanthanum Strontium Manganese oxide (LSMO) nanoparticles are a new class of magnetic nanoparticles, which exhibit favorable magnetic and biological properties for therapy using hyperthermia, imaging and diagnosis; opening avenues for multimodal anti-cancer therapy. Ease of synthesis and facile surface modifications makes LSMO nanoparticles a promising candidate for its application in anti-cancer therapy.

Introduction

Cancer is a disease involving complex pathogenesis an often develops over many years through a multistage process involving spurring and accumulation of several

molecular abnormalities [1,2]. The disease involves multiple pathway crosstalk [3–5], metastatic capability[6,7] and drug resistance[8–10] that limit treatment outcomes. Detection of cancer at an early stage of disease progression is a very important to increase the success of clinical treatment [11]. Currently, cancer is detected using various medical tests such as blood, urine, or imaging techniques followed by biopsy. Conventional anatomical imaging techniques typically detect cancers when they are few millimeters (e.g., MRI) or centimetres (e.g., PET) in diameter, at which time they already consist of more than a million cells. In the clinic, conventional therapies such as surgery, chemotherapy and radiation (alone or in combination) are often inadequate to ensure complete removal of tumor and preventing relapse when the cancer has progressed to higher grade. Further, conventional therapies are also known to result in undesirable side effects. Hence, alternative remedies (with no or lesser side effects) and early diagnosis can be useful in management of cancer. Recently proposed molecular imaging aims at rectifying this disadvantage. The development of this new imaging modality became possible due to the recent progress in nanotechnology, molecular and cell biology, and imaging technologies. While molecular imaging applies to various imaging techniques such as Positron Emission Tomography (PET), computed tomography (CT), or ultrasound, of particular interest is magnetic resonance imaging (MRI) that provides the best spatial resolution when compared to other techniques and is noninvasive or at least minimally invasive.

Unfortunately, MRI has not been applied to its full potential for the diagnosis of cancer mostly because of its low specificity. MRI specificity can be enhanced using cell markers and unique properties of paramagnetic and superparamagnetic nanoparticles (NP). Superparamagnetic nanoparticles when placed in the magnetic

field disturb the field causing faster water proton relaxation, thus enabling detection with MRI.

Under normal conditions protons or hydrogen nuclei in the water molecules in the body are spinning about their axes and are randomly oriented. When an external magnetic field, B_0 is applied the nuclear spins align with the field and also around the axis of the external magnetic field producing a net magnetic moment, M. Upon application of a RF pulse to the object to be imaged causes the nuclear spins to be away from the z-axis and these excited spins start aligning in the transverse plane. When the pulse is switched off the net magnetic moment, M continues to wobble, giving off RF waves and hence producing NMR signal. The protons recover their original state of equilibrium by two relaxation processes namely T1 and T2 to generate an MR image.

Nanotechnology, as a science, has often been prophesied to revolutionize cancer management by developing nanoparticles for early detection of cancer *in vivo*, its rapid molecular analysis *ex vivo* and subsequent anti-cancer therapy [12].

Cancer therapies can be broadly classified as local (e.g. surgery and radiotherapy) or systemic (e.g. chemo- and hormone -therapy). Breast tumors are commonly removed by partial or total mastectomy. Mastectomy is a preferred treatment option since it does not have hamper any vital functions of the body, and is known to reduce the chances of a relapse. Systemic therapies are essentially adjuvant therapies aimed at controlling metastasis.

In many clinical cases, conventional therapies often fail to ensure complete removal of tumor and prevent relapse. Besides some of these treatments are known to cause undesirable side effects. Temporary effects of breast cancer treatment wear off eventually after treatment is stopped.

Magnetic nanoparticles (MNPs) by far are the most explored nanoparticle system in this particular aspect [13]. They show potential applications not only in therapy, but also in imaging and diagnostics. Drug delivery, magnetic resonance imaging (MRI), hyperthermia, bio-separation and bio-sensing are few bio-medical applications of MNPs [14–18]. Specifically, MNPs have contributed significantly for development of theranostics for cancer by their active and passive drug and gene carriers [19,20], as contrast agents in tumor visualization [21–23], magnetic separation of cancer cells [24–26] or detection tags in diagnosis of cancer biomarkers [27]. One of the unique ability of MNPs is heating under radio frequency radiation and, in turn elevating temperature of immediate surrounding [17,28,29]. This property of MNPs has been widely explored for their use as hyperthermia agents, in treatment of cancer by using applied heat to destroy tissue or make cancer cells more susceptible to conventional therapies *in vitro* and *in vivo* [30–33].

Depending on their size and surface, nanoparticles can target the tumour either passively and/or actively in order to deliver contrast agents and drugs. Passive targeting makes use of the leaky and porous tumour vasculature, which enables the macromolecules and nanoparticles to accumulate in the interstitial spaces. In addition, the disturbed vessel leads to reduced lymphatic drainage from tissue resulting in enhanced local concentration of nanoparticles. Active targeting is achieved by conjugating nanoparticles with targeting molecules such as ligands having high affinity towards unique cell surface receptors or antigens on tumour cells. Nanoparticles can penetrate through small capillaries and are taken up by cells, which allow efficient drug accumulation at target sites enabling also a sustained and controlled release of drugs at target sites over a period of days or even weeks. In

general, drug targeting by nanoparticles or nanocapsules reduces dosage, ensures the pharmaceutical effects, minimizes side effects, and enhances drug stability.

Conventional anti-cancer treatments have limited therapeutic efficacy owing to complex nature of cancer pathogenesis, metastasis and drug resistance. Therefore, newer alternatives are the need of the day.

Hyperthermia is one such alternative therapy that uses heat (typically, 41-48°C) to treat cancers. Non-cancerous cells are characteristically more resistant to elevated temperatures in comparison to cancerous ones; since normal tissues can dissipate heat via circulating blood. However, tumors tend to accumulate heat because of their low and sluggish perfusion status. This accumulated heat causes physical injury at multiple levels, leading to cell membrane and cytoskeletal damage. The membrane fluidity and potential also gets affected after hyperthermia; and molecular changes viz. damage to intercellular proteins, generation of reactive oxygen species, increase in levels of heat shock proteins and damage to mitochondrial membrane are observed. Hyperthermia also provokes induction of cytostatic signals and temporary arrest of cell division. Further, hyperthermia results in generalized destruction of microvessels in the tumor and also inhibits neo-angiogenesis. Loss of vasculature can cause loss of tumor drainage leading to oxygen and nutrient depletion, thereby arresting tumor proliferation.

Hyperthermia can be administered either to the whole body or locally (i.e. at tumor site) to treat cancer. Heat is applied by hot water perfusion or microwave heating or through heating probes inserted in the tumor. External application of heat (using methods such as hot water perfusion and microwave heating) is not preferred owing to its non-specificity and inability to deliver heat to deep-seated cancers. Hence, the focus has shifted to more directed (localized) methods such as insertion of heat

applicators at the tumor sites. Various surgically implanted materials such as microwave antennas, radiofrequency electrodes, ultrasound radiators, voltage driven resistance wires, magnetic 'seeds', infra-red radiators have been used for localized heating. Smaller sized hyperthermia mediators such as magnetic seeds also require implantation in the tumor tissue. However, insertion as well as removal of such probes requires surgical intervention that may not be always desired.

Nano-sized materials capable of heating with external energy have emerged as a new class of hyperthermia agents that do not require surgical intervention. For example, gold nanoparticles have been observed to heat up with infrared radiation and act as hyperthermia agents. However, relatively small depth of penetration of the infrared (IR) radiation limits its therapeutic applicability. Another concern is possible damage to surrounding healthy tissue due to uncontrolled heating.

Hyperthermia can also be achieved by using magnetic nanoparticles (MNPs) that get heated up on exposure to radiofrequency radiation (100 kHz to 400 KHz) and raise the temperature of tumor tissue. It is known that heating is directly proportional to the radiation frequency used, which can be exploited to achieve proper temperature control, finally leading to cell death. Radiofrequency mediated hyperthermia is considered as safer than IR-based hyperthermia.

Magnetic fluids (i.e. magnetic nanoparticles dispersion in liquid media) when exposed to radiofrequency field can cause heat generation by several processes viz. Neel and Brownian relaxation, hysteresis loss and frictional losses (in viscous suspensions). Magnetic materials contain "domains" that align in response to an applied external magnetic field. On removal of the magnetic field, the magnetic moments revert back to their original state. This process of magnetic moment alignment and reversal causes heat generation. In case of alternating magnetic field (radiofrequency), there is cyclic

reversal of the magnetic field ensuring continuous heat generation. This process can be used to heat up the cells in hyperthermia application.

In case of superparamagnetic nanoparticles such as iron oxide nanoparticles, Néel's and Brownian relaxation are the predominant mechanisms involved in generating heat. Néel's relaxation is a function of the spin of the magnetic nanoparticle, i.e. when the magnetic field is reversed heat is generated by relaxation of magnetic moment of the particle. Brownian relaxation denotes that magnetic nanoparticles physically rotate under the alternating magnetic field and generate heat due to friction within the carrier liquid.

Heating of magnetic nanoparticles by radio frequency is also a function of the Curie temperature that is governed by their magnetic and electron transport properties. Curie temperature is an important parameter in selection of magnetic material for an in vivo application like hyperthermia. On exposure to radiofrequency, magnetic nanoparticles get heated up as long as the temperature is below their Curie temperature. Once the Curie temperature is reached, the saturation magnetization of particles drops to zero, and heating stops as the material becomes purely paramagnetic (termed as "self-controlled heating"). Studies indicate that heating efficiency of MNPs also varies with composition, route of synthesis, size and whether they are single/multi domain in nature. Thus, if the Curie temperature can be fixed by judicious selection of particle composition and size, hyperthermia can be safely applied. The dosage not only is dependent on the system in use, Curie temperature or external RF parameters, but also is dependent on the specific absorption rate (SAR) of the tissue. High SAR is essential to heat the tissue for rapid action of killing of tumor cells. The dosage is selected in such a way that maximum SAR is obtained to efficiently suppress tumor.

Different MNPs reported for magnetic fluid hyperthermia, bio-separations and magnetic resonance imaging include superparamagnetic iron oxides [34] and ferrites of manganese, cobalt, nickel and zinc, etc. [35]. A relatively new class of magnetic nanoparticles, Lanthanum strontium manganese oxide (LSMO) nanoparticles has recently been explored for similar use in anti-cancer therapy. This review summarizes the recent work on LSMO nanoparticles in therapeutics and diagnostics with a special focus on LSMO nanoparticle mediated hyperthermia for cancer therapy.

Properties of LSMO nanoparticles

LSMO nanoparticles are manganese oxide based compounds (manganites) with the formula R1-xAxMnO3; where the R sites are substituted by the rare earth metal-lanthanum, and A by strontium, which is a divalent alkaline earth metal The LSMO crystal is a perovskite-structured oxide, which is generally ferromagnetic in bulk form. However, super-paramagnetic and ferromagnetic nanoparticles of LSMO have been reported widely in literature.

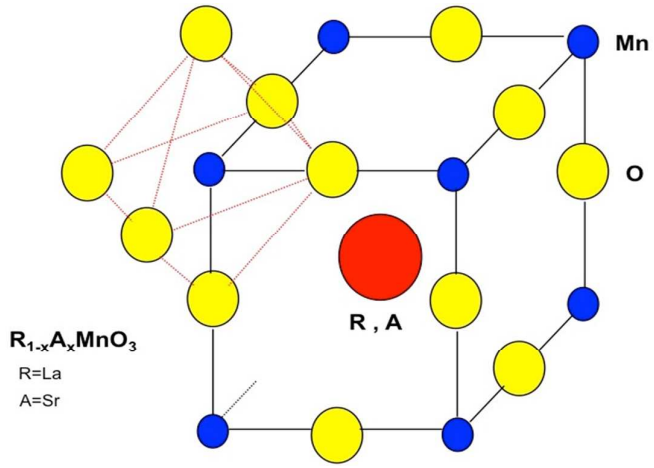

Figure 1: Structure of a typical LSMO perovskite structured oxide.

Synthesis and surface modifications of LSMO nanoparticles

The properties of LSMO nanoparticles like grain formation and annealing, magnetic properties, particle size and homogeneity are greatly dependent on the route of synthesis. When nanoparticles are to be obtained from bulk form of LSMO (e.g. by mechanical grinding post synthesis) i.e. when a top-down approach is implemented, the nanoparticles may have a broad size distribution, variation in the individual grain sizes and their geometries. While in the bottom up approach (e.g. chemical reduction of salts or decomposition based synthesis), the reaction and nanoparticle formation can be tailored by controlling the chemistry of reaction and nanoparticle organization. This gives an option of engineering properties, reducing aggregation and introducing different surface functionalities.

Several methods reported to synthesize LSMO nanoparticles include glycine nitrate combustion, chemical synthesis, sol-gel, citrate gel method, etc. [36–40]. The synthesis method governs properties of nanoparticles such as grain formation and annealing, magnetism, size and homogeneity. Hydrothermal synthesis of LSMO nanoparticles involves high temperature and pressure treatment to precursors in aqueous solution to form nanoparticles, addition of various surfactants during synthesis can help achieve particle size control [41]. Combustion method is a relatively faster synthesis method involving use of an organic molecule (with low decomposition temperature) that acts like a fuel in the synthesis procedure [42,43]. Chemical methods have been widely used to synthesize LSMO nanoparticles for biomedical uses, since standardized conditions of pH, temperature and reactant stoichiometry ensure chemical homogeneity [44,45]. Sol gel methods reportedly produce small sized LSMO nanoparticles, and allow control over the size and crystallinity [46,47]. Thermal decomposition method for synthesis for nanocrystalline LSMO is a quick and easy method (Daengsakul et al. 2009).

Ravi and Karthikeyan [36] have recently described modified sol gel method where LSMO nanoparticles were synthesized using an oleic acid surfactant and a polyacrylic acid matrix. It was observed that temperatures up to 500 ・C generated paramagnetic, while at 800 ・C produced ferromagnetic LSMO nanoparticles. Although the size of the nanoparticles did not vary significantly (20-30 nm), calcination temperatures affected the magnetic properties.

LSMO nanoparticles synthesized using polyvinyl alcohol (50-60 nm) and glycine (40-50 nm) show magnetization of 34.9 and 54.9 emu/g, respectively [48]. In another study, a non-aqueous sol gel method was used to produce 20 nm particle with high saturation magnetization values; here, formation involved C-O bond breaking and formation the metal oxide bond without any hydrolysis [37].

Magnetic nanoparticles in biomedicine can be used for an array of applications including hyperthermia, magnetic resonance imaging, and drug delivery. Such applications require a stable, colloidal suspension of magnetic nanoparticles in a non-toxic solvent to facilitate injection [49] as well as their circulation of nanoparticles *in vivo.* However, many magnetic nanoparticles, including LSMO nanoparticles, are not dispersible in aqueous solutions and show gradual aggregation and settling. Hence, it was thought essential to tune the LSMO surface such that it renders them colloidal. Surface modifications by diverse approaches have been attempted to make stable magnetic nanoparticle suspensions. Magnetic nanoparticles can be surface engineered during synthesis or they can be modified after synthesis to enhance their functions [50]. Modifications of magnetic nanoparticles using polymers, gold, silver, copper, carbon, silica or even small fluorescent nanoparticles etc. have been attempted to improve

their stability, surface chemistry and functionality [51]. Surface coatings can be used to impart positive charge on negatively charged nanoparticles. It has been reported that positively charged nanoparticles are more successful at crossing the cell membrane barrier than neutral or negatively charged ones [52]. Further, coating can improving surface reactivity to carry therapeutic moieties like drugs and ligands; and in certain cases reduce toxicity [27].

Biocompatible molecules like bovine serum albumin (BSA) and dextran sulfate have been immobilized on LSMO by covalent and electrostatic interactions, respectively; and these coatings have increased the compatibility of LSMO in biological systems. BSA was conjugated to LSMO using linker and the size of nanoparticles ranged from 80-100 nm, dextran coated LSMO show a size of 30-35 nm. The magnetization of LSMO was 14 emu/g in case of BSA conjugated and 30 emu/g for dextran coated ones [53]. Along with contributing to biocompatibility, coating with dextran imparts a near-neutral charge to LSMO nanoparticles thus decreasing their interactions with other biomolecules. It could be possible that their overall internalization in cells is lower than charged nanoparticles, which is responsible for reduction in toxicity [54]. LSMO coated with chitosan showed good colloidal stability and biocompatibility up to concentration of 1 mg/ml [55]. Other strategy is coating the magnetic nanoparticle with a stabilizing agent or generating a core-shell like structure. Stabilizing LSMO during synthesis is possible by using bilayer oleic acid surfactant mediated synthesis; these bilayer coated nanoparticles did not show aggregation in conditions of physiological pH and at high ionic strength [56]. Oleic acid (OA) functionalized surfaces have been further modified using a polymeric shell of Pluronic F127 to generate core shell structures with good dispersibility and a high SAR value for hyperthermia based applications [57]. In another study, OA-betaine HCl functionalized

LSMO nanoparticles were synthesized, betaine HCL was used as a second surfactant to make the preparation more biocompatible and adds amphiphilic nature to nanoparticles [58]. Apart from polymer and biomolecule shells to impart stability and biocompatibility, LSMO nanoparticles with inorganic shells generate materials with enhanced chemical stability as well as favorable surface chemistry for modification. Superparamagnetic LSMO cores with gold shells can be used for hyperthermia and surface drug attachment using amine/thiol terminal groups from shell [59].

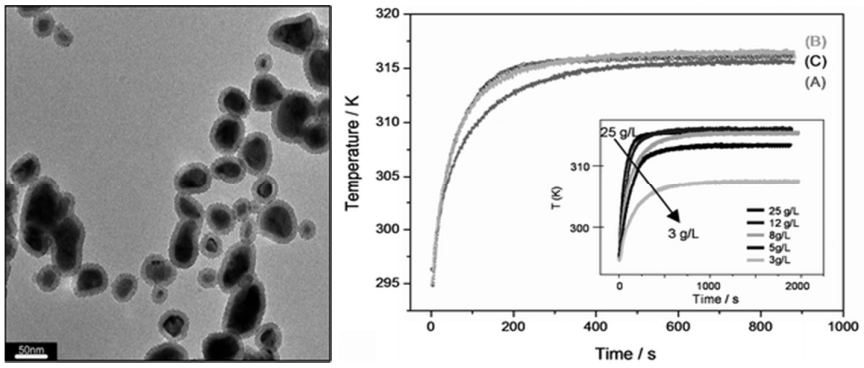

Figure 2: a) LSMO@silica nanoparticles synthesized using glycine nitrate process and coated with silica post synthesis and b) Heating experiments ([Mn] = 25 g L^{-1} at 108 kHz for (A) LSMO in agarose, (B) LSMO@silica in agarose, and (C) LSMO@silica in water. Inset - magnetic heating experiments for LSMO (88 mT, 108 kHz) *vs.* manganese concentration [42].

LSMO nanoparticles for magnetic fluid hyperthermia

Hyperthermia is rise in temperature above physiological range; it has been practiced since ancient times to alleviate diseases. The aim of hyperthermia is to raise the temperature of tumor sufficiently enough to instigate cell death. Magnetic nanoparticles (MNPs) get heated up on exposure to radiofrequency radiation and raise temperature of tumor tissue [17,28,29]. Contingent with their sizes and magnetic

properties, MNPs can be divided into superparamagnetic and ferromagnetic. Super-paramagnetic nanoparticles do not show residual magnetization and coercivity unlike ferromagnetic and are generally preferred as hyperthermia mediators. Super-paramagnetic LSMO nanoparticle exhibit zero magnetism in absence of an external magnetic field. However, when a radio frequency radiation is provided, they utilize this energy to re-orient their magnetic moments, generating thermal vibrations in the surrounding medium. The mechanisms involved in generating this heat can be Néel's and Brownian relaxation or hysteresis loss. Hysteresis loss and Eddy loss is generally seen in ferromagnetic materials whereas super-paramagnetic materials show Brownian and Néel's relaxation. By Brownian relaxation, these nanoparticles physically rotate under the alternating magnetic field and generate heat by friction. Néel's relaxation is a function of the spin of the magnetic nanoparticle, that is, when the magnetic field is reversed heat is generated by relaxation of magnetic moment of the particle [60].

Heat generation from magnetic particles is dependent on its specific absorption rate (SAR) or, specific loss power (SLP). When the absorption rate or loss power of the magnetic particles is high, the dose of nanoparticles required for hyperthermia can be reduced. Studies indicate that heating of MNPs varies with composition, route of synthesis, sizes and whether they are single/multi domain in nature [60]. The Curie temperature (T_c) is another important parameter in selection of magnetic material for an *in vivo* application like hyperthermia. It is the temperature above which magnetic materials get converted to paramagnets. As long as the particles are below their Curie temperature, they are heated when the AC field is applied. Once they reach the Curie temperature, the saturation magnetization of particles drops to zero, and heating stops as the material becomes purely paramagnetic. Thus, if the Curie temperature can be

fixed by judicious selection of particle composition and size, hyperthermia can be applied and carefully controlled [61].

Curie temperature of LSMO nanoparticles synthesized by different routes show acceptable range and can be used for hyperthermia safely [42,62–65]. Curie temperature of LSMO synthesized by various routes and coated with different coating materials fall into an acceptable range and can be used as hyperthermia agents safely. Curie temperature of 335 K was reported by Kaman et al [66]; Curie temperature of acrypol coated LSMO is 318 K [64], octadecyl amine (ODA) and fatty amine coating show 360 K [67] while LSMO synthesized using aqueous combustion route read 316 K [42]. However, along with the increasing interest in treatment of cancer using an effective patient friendly approach like hyperthermia there is also a rising concern with use of the conventional hyperthermia agents- iron oxide nanoparticle. Iron oxide nanoparticles generally show high Curie temperature [34]; and additionally add to iron homeostasis and toxicity concerns [68] Thus advantage of 'self-controlled' heating in desirable range can establish LSMO nanoparticles as superior hyperthermia mediator in comparison to its counterparts [62,69].

In our studies, LSMO nanoparticle synthesis was carried out using a thermal decomposition method [70] with modifications. LSMO nanoparticles when exposed to a field of 365 kHz, showed temperature of ~51±0.7°C was obtained for 1, 2 and 5 mg/ml nanoparticles in 20, 10 and 6 min respectively (Figure 3). The heating profile showed that temperature rise is concentration dependent. The temperature rise for all tested concentrations gained platitude after 20 min of RF exposure. It can be safely said that varying the concentration and time of exposure for hyperthermia treatment, desired temperature can be administered to cancerous cells (Kulkarni et al., 2015).

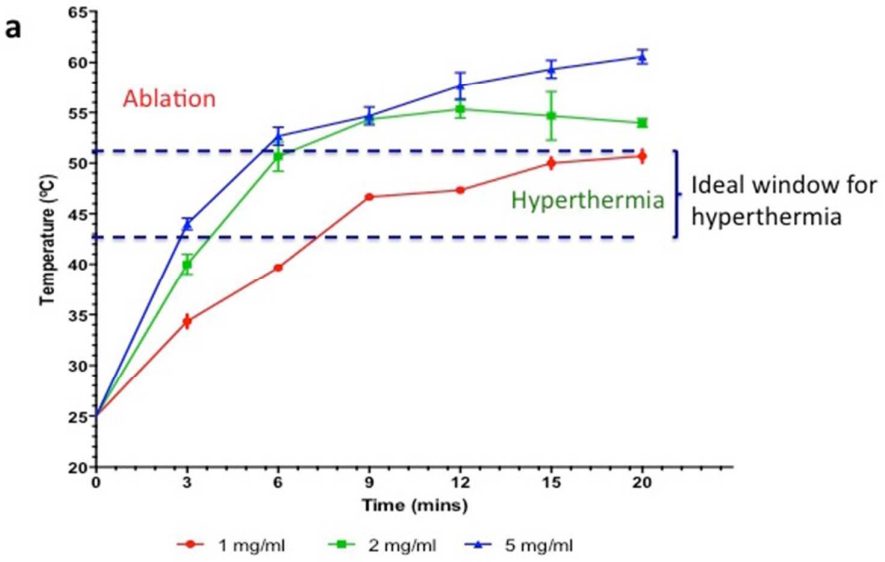

Figure 3. Heating profile of LSMO nanoparticles synthesized by thermal decomposition method (Kulkarni et al., 2015)**.**

Tumors tend to accumulate heat within because of their low and sluggish perfusion [71–73]. Vascularization is affected by hyperthermia, neo-angiogenesis is also inhibited along with generalized destruction of microvessels in tumor [74,75]. Physical injury by heat causes multiple levels of damage, leading to mutilation of cell membrane and cytoskeleton [76,77]. The membrane fluidity and potential gets affected after hyperthermia [78]; and molecular changes like damage to intercellular proteins, generation of reactive oxygen species, increase in levels of heat shock proteins and damage to mitochondrial membrane has also been reported [79–82]. Transient heat treatments induce cytostatic processes where the cell temporarily gets arrested and division halts [80]. When dextran stabilized nanoparticles were used for hyperthermia treatment of human melanoma cell line- change in morphology, proliferation pattern and expression of heat shock proteins 70 and 90 were observed [83].

LSMO nanoparticles based hyperthermia could be an alternative therapy that is targeted with no or less side effects and more patient-friendly than chemo- and radiotherapies with dose-dependent side effects. As surgery shows poor patient acceptability, solid tumors can be treated by nanoparticle based hyperthermia to avoid invasive operations [84].

Drug loading and combinatorial therapy using LSMO nanoparticles

Apoptosis in cancer cells post treatments like chemotherapy, radiation and hyperthermia have already been studied extensively [85]. Along with hyperthermia as a standalone therapy, many clinical trials have shown improved benefits of hyperthermia when applied alongside chemo- and radiotherapy. Studies report that sluggish perfusion of tumors can be transiently improved by hyperthermia [86,87], which can help to deliver chemotherapeutic drugs. Hyperthermia has been reported to enhance the effects of anti-cancer drugs in different types of cancer, including sarcoma, breast cancer, etc. [88–90]. In other studies, combinatorial therapy of hyperthermia and chemotherapy was found to increase lifespan of gastric and ovarian cancer patients [91–93]. In a Phase III study on patients with advanced cervical carcinoma, combination of radiotherapy, chemotherapy, and hyperthermia showed a 15% improvement in overall survival as compared to conventional treatment [94]. Hyperthermia in conjunction with radiotherapy displayed better results than radiotherapy alone in glioblastoma, prostrate- and cervical- cancer patients (Heijkoop et al. 2012; Franckena 2012; Hurwitz et al. 2011; Maier-Hauff et al. 2007). The hypoxic and quiescent cells within the tumor structure are resistant to radiotherapy. However these cells are more heat-sensitive, hence it has been observed that hyperthermia sensitizes these hypoxic and quiescent cells to radiation damage emphasizing on the advantages of combination therapy [99].

A concern with use of chemotherapeutics like doxorubicin, lies in the dosage dependent cardiotoxicity[100], hepato- and nephrotoxicity[101] resistance of cancer cells to high doses of drugs [102]. Magnetic drug targeting is an attractive option to restrict or localize the activity of the drug to the site of interest. In case of chemotherapeutic drugs prescribed for cancer, such targeting can significantly contribute by reduction in drug-associated toxicity in healthy tissue and at the same time increase the concentration of pharmacologically active agent at target site. Multiple approaches for drug loading can be adopted using LSMO nanoparticles; either the drug can be covalently or electrostatically presented on surface, or the nanoparticles and drugs can be encapsulated together. An applied external magnetic field can ensure that maximum nanoparticles are retained at tumor site and heating of nanoparticles can trigger release of drug. Silica coated LSMO nanoparticles modified with block co-polymer structures (poly l-lysine and polyether segments) have used this strategy of encapsulating hydrophobic drugs like doxorubicin for thermally triggered drug release [103]. Doxorubicin loaded on chitosan coated LSMO nanoparticles has been used as drug delivery and hyperthermia agent in treatment of breast cancer cells *in vitro*. Primary coating of LSMO nanoparticles with positively charged polymer chitosan increased their colloidal stability and prepared the nanoparticle surface for doxorubicin loading. The nanoparticle system could release drug on stimuli of radio frequency radiation (Figure 4) (Kulkarni et al., 2015). In another report, Paclitaxel was encapsulated in a hybrid magnetic nanovesicle containing dextran coated LSMO and iron oxide; this system could be used for combined hyperthermia and chemotherapy. This ‘biphasic’ nanovesicles encapsulated ~83% of drug and a

combined effect of hyperthermia and chemotherapy was seen on human breast cancer cells MCF-7 [104].

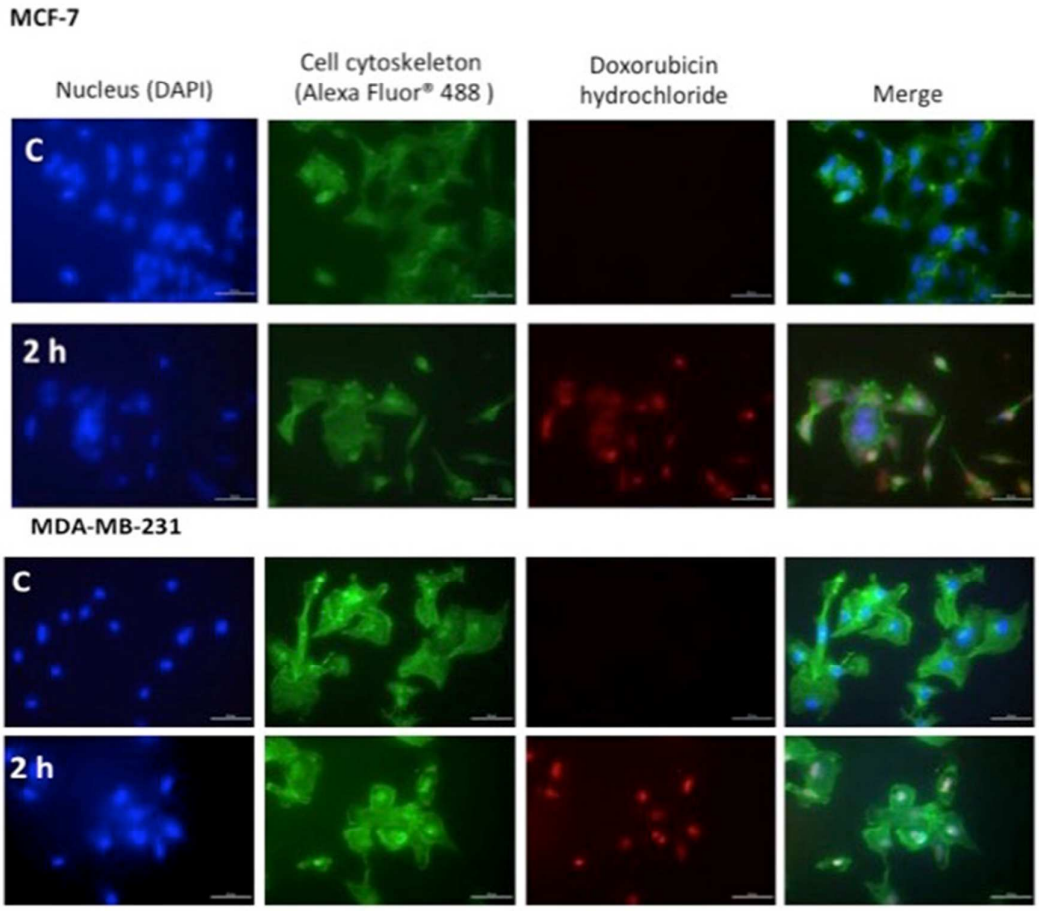

Figure 4: Doxorubicin release and its nuclear accumulation from chitosan coated LSMO nanoparticles post radiofrequency radiation in human breast cancer cell lines MCF-7 and MDA-MB-231 (Kulkarni et al., 2015)

As chemotherapy is a relatively nonspecific therapy, trigger-based release along with a potent combination therapy can be a promising attempt at reducing drug-associated drawbacks.

Fluorescence imaging and MRI contrast agents

LSMO core structure with double layer shell of fluorescent alkoxide/tetraethoxy silane and tetraethoxy silane could function as fluorescent probes in cell imaging and also as an MRI contrast agent. These nanoparticles bear a manganite core ~57 nm and an overall diameter of ~89 nm. The excitation maximum of these nanoparticles was seen to be 514 nm and the emission maximum corresponded to that of fluorescein. Along with their fluorescence, these nanoparticles also showed high spin-spin relaxivities (r_2 = 580, 540 and 520 $s^{-1}mmol(Mn)^{-1}$ L at magnetic fields of 0.5, 1.5 and 3 T, respectively) which exceeded the relaxivity reported for iron oxide [105]. Similar studies show that LSMO surface modified with SiF@Si along with fluorescent probe could be successfully used for cell labeling and contrast agent [106]. In MRI, a magnetic field is applied followed by a magnetic pulse provided to sample, and the change in magnetization of protons in water molecules is measured. Protons will relax differently depending on the source (tissue) they belong to, hence providing a contrast enabling differential visualization. This relaxation process involves the longitudinal relaxation time T1; and a transverse relaxation time, T2. Although MRI can efficiently image anatomical details, using magnetic contrast agents help change the relaxation of water in their vicinity and improve differential visualization. Since the magnetic single domains have a magnetic moment, they are surrounded by a magnetic field produced from the magnetic moment. This surrounding magnetic field interacts with the hydrogen nucleus in the water molecules in the body and thereby affects the resonance properties. Tools like MRI can help improving the detection of cancers and their metastases. There are T1 and T2 contrast agents; and Gadolinium (Gd), super-paramagnetic iron oxide nanoparticles (SPIONs) have been conventionally used as MRI agents. Recently, dextran stabilized $La_{0.7}Sr_{0.3}MnO_3$ nanoparticles (Dex-LSMO

NPs) have been used as a new type of contrast agents which have been established safe and compatible for *in vivo* use.

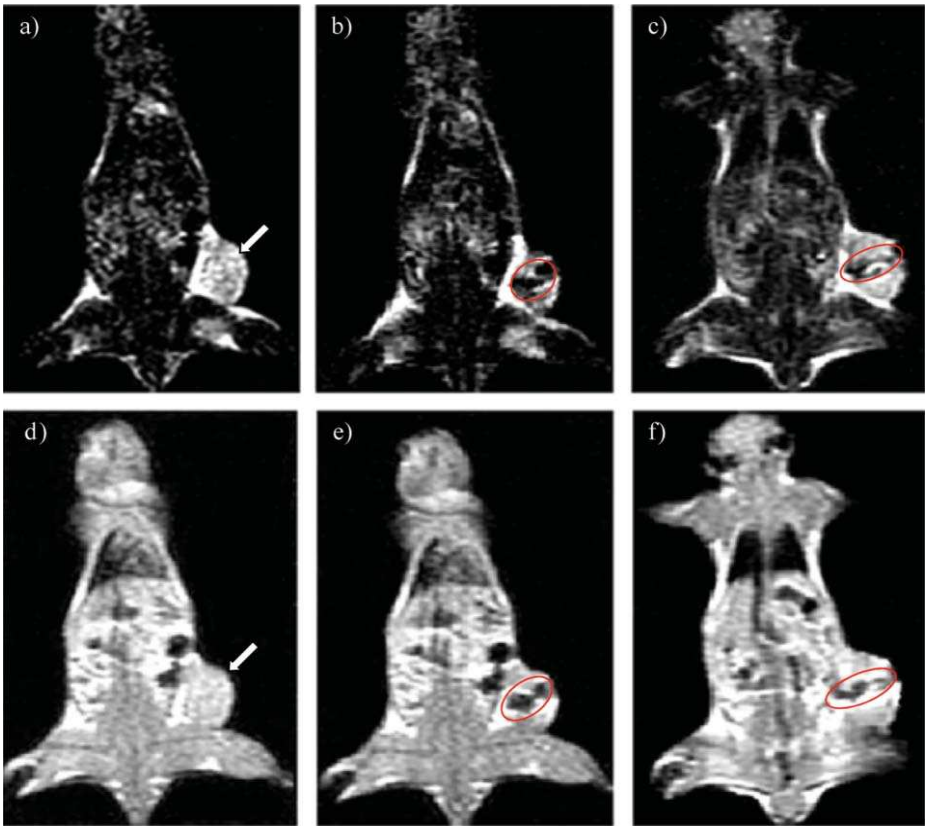

Figure 5: B16F1 melanoma bearing mice showing T2 weighted images a) before Dex-LSMO injection, b) 15 min post Dex-LSMO injection, c) 24 h post injection; T1 weighted images d) before injection of Dex-LSMO, e) 15 min post Dex-LSMO injection and f) 24 h post injection of Dex-LSMO injection [107].

Dex-LSMO NPs showed both positive and negative contrast properties; with r2 value of 778 s−1 mg−1 mL [107]. This opens up the possibilty of image directed hyperthermia using LSMO nanoparticles in future.

Förster resonance energy transfer (FRET) using LSMO nanoparticles

Förster resonance energy transfer (FRET) is energy transfer between two molecules i.e. a donor and an acceptor molecule. FRET is very a very sensitive technique and can be used for measurements, determination of distances between the participating molecules. Interactions of modified LSMO with other biomolecules can be conducted using Förster resonance energy transfer (FRET) studies; citrate stabilized LSMO were used to study interaction of covalently bound chromophore 4-nitrophenylanthralinate (NPA) and adsorption of fluorescent adenine analogue (AP) on nanoparticle surface [108].

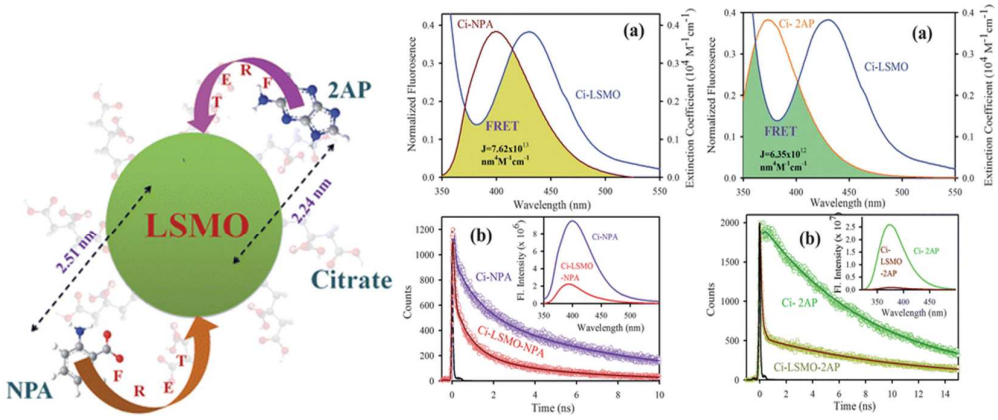

Figure : a) Schematic showing covalent attachment of NPA and non-covalent adsorption of base analogues 2AP with FRET transfer from ligands to nanoparticles b) Spectral overlap between the citrate NPA donor - citrate LSMO acceptor (above) and the quenching of donor (below, and inset). Excitation wavelength- 320 nm for steady state, and 375 nm for time resolved experiments; c) Spectral overlap between the citrate 2AP donor - citrate LSMO acceptor (above) and the quenching of donor (below, and inset), excitation wavelength- 300 nm [108].

As MR imaging and FRET analysis using modified LSMO nanoparticles is possible, they can be used for diagnosis of cancer biomarkers and whole cells *in vivo*.

Conclusions and future outlook

Efficient yet minimally invasive therapies showing fewer side effects, like magnetic fluid hyperthermia, are gaining impetus since the last decade. The driving force for patients opting towards such alternative therapies include the drug associated resistance shown by cancer cells, dosage dependent side effects on healthy cells and the rate failure of conventional therapies. The potential of LSMO nanoparticles, with their attractive magnetic properties and an inherent biocompatibility, has already been established with studies demonstrating its therapeutic efficiency.

Table 1: Biomedical applications of LSMO nanoparticles.

YEAR	AUTHOR	APPLICATION	REF NO.
2010, 2015	Kačenka et. al.	Hybrid silica- fluorescein layer coated LSMO nanoparticles for imaging	105, 109
2013	Berkova et. al.	Silica oated LSMO nanoparticles for MRI	110
2013	Bhayani et. al.	Dextran coated LSMO nanoparticles for hyperthermia	12
2013	Thorat et. al.	Oleic acid coated LSMO nanoparticles for hyperthermia	43
2013, 2015	Jadhav et. al.	Polyvinylpyrrolidone glycol coated and Polyvinyl alcohol, polyethylene glycol coated LSMO nanoparticles for hyperthermia	111, 112

2014	Manh et. al.	LSMO nanoparticles for hyperthermia	[113]
2014	Shete et. al.	Chitosan coated LSMO nanoparticles for hyperthermia	[114]
2013, 2015	Haghniaz et.al.	Dextran coated LSMO nanoparticles for hyperthermia and MRI	[107, 115]
2015	Veverka et. al.	Silica coated LSMO nanoparticles for MRI	[116]

LSMO nanoparticles can be categorized as theranostic agents; i.e. they function as MRI contrast agents as well as a heat-generating source for localized hyperthermia. Along with hyperthermia and imaging, LSMO can also act as drug delivery agent. These review summarized initial work conducted in the field of biomedicine using these relatively fresh magnetic nanoparticle system. *Prima facie*, we can comprehend that these nanoparticles have the potential to go a long way in biomedicine owing to their ease of control over size, magnetism and heating. It would be interesting to further investigate LSMO nanoparticles for simultaneous hyperthermia, drug delivery and contrast agent for all round cancer theranostics. A comprehensive study on their *in vivo* residence and clearance times, effectiveness of anti-tumor therapy in animal models is warranted to develop LSMO nanoparticles as nanomedicines.

Acknowledgment

VK is grateful to the Council of Scientific and Industrial Research (CSIR), India for the award of funds.

Reference:

1 I. B. Weinstein and A. K. Joe, *Nat. Clin. Pract. Oncol.*, 2006, **3**, 448–57.

2 B. Vogelstein and K. W. Kinzler, *Nat. Med.*, 2004, **10**, 789–99.

3 D. Hanahan and R. A. Weinberg, *Cell*, 2011, **144**, 646–74.

4 C. H. Squarize, R. M. Castilho, V. Sriuranpong, D. S. Pinto and J. S. Gutkind, *Neoplasia*, 2006, **8**, 733–46.

5 E. F. Wagner and A. R. Nebreda, *Nat. Rev. Cancer*, 2009, **9**, 537–49.

6 G. P. Gupta and J. Massagué, *Cell*, 2006, **127**, 679–95.

7 I. J. Fidler, *Nat. Rev. Cancer*, 2003, **3**, 453–8.

8 M. Dean, T. Fojo and S. Bates, *Nat. Rev. Cancer*, 2005, **5**, 275–84.

9 A. Singh and J. Settleman, *Oncogene*, 2010, **29**, 4741–51.

10 M. M. Gottesman, *Annu. Rev. Med.*, 2002, **53**, 615–27.

11 T. Green, K. Atkin and U. Macleod, *Br. J. Cancer*, 2015, **112**, S41–S49.

12 M. Ferrari, *Nat. Rev. Cancer*, 2005, **5**, 161–71.

13 Q. A. Pankhurst, J. Connolly, S. K. Jones and J. Dobson, *J. Phys. D. Appl. Phys.*, 2003, **36**, R167–R181.

14 R. Banerjee, Y. Katsenovich, L. Lagos, M. McIintosh, X. Zhang and C.-Z. Li, *Curr. Med. Chem.*, 2010, **17**, 3120–3141.

15 N. Tran and T. J. Webster, *J. Mater. Chem.*, 2010, **20**, 8760.

16 S.-H. Huang and R.-S. Juang, *J. Nanoparticle Res.*, 2011, **13**, 4411–4430.

17 A. Singh and S. K. Sahoo, *Drug Discov. Today*, 2014, **19**, 474–81.

18 M. V Yigit, A. Moore and Z. Medarova, *Pharm. Res.*, 2012, **29**, 1180–8.

19 S. Prijic and G. Sersa, *Radiol. Oncol.*, 2011, **45**, 1–16.

20 F. M. Kievit and M. Zhang, *Acc. Chem. Res.*, 2011, **44**, 853–62.

21 Y. Cheng, R. A. Morshed, B. Auffinger, A. L. Tobias and M. S. Lesniak, *Adv. Drug Deliv. Rev.*, 2014, **66**, 42–57.

22 M. Wankhede, A. Bouras, M. Kaluzova and C. G. Hadjipanayis, *Expert Rev. Clin. Pharmacol.*, 2012, **5**, 173–86.

23 J. E. Rosen, L. Chan, D.-B. Shieh and F. X. Gu, *Nanomedicine*, 2012, **8**, 275–90.

24 S.-M. Jo, S. Noh, Z. Jin, Y. Lim, J. Cheon and H.-S. Kim, *Sensors Actuators B Chem.*, 2014, **201**, 144–152.

25 J. O. Fierer, G. Veggiani and M. Howarth, *Proc. Natl. Acad. Sci. U. S. A.*, 2014, **111**, E1176–81.

26 W. Lu, M. Ling, M. Jia, P. Huang, C. Li and B. Yan, *Mol. Med. Rep.*, 2014, **9**, 1080–1084.

27 O. Veiseh, J. W. Gunn and M. Zhang, *Adv. Drug Deliv. Rev.*, 2010, **62**, 284–304.

28 D. Ruiz-Molina, F. Novio and C. Roscini, Eds., *Bio- and Bioinspired Nanomaterials*, Wiley-VCH Verlag GmbH & Co. KGaA, Weinheim, Germany, 2014.

29 R. Regmi, A. Naik, J. S. Thakur, P. P. Vaishnava and G. Lawes, *J. Appl. Phys.*, 2014, **115**, 17B301.

30 S. Dutz and R. Hergt, *Nanotechnology*, 2014, **25**, 452001.

31 S. Kossatz, R. Ludwig, H. Dähring, V. Ettelt, G. Rimkus, M. Marciello, G. Salas, V. Patel, F. J. Teran and I. Hilger, *Pharm. Res.*, 2014, **31**, 3274–88.

32 P. T. Yin, B. P. Shah and K.-B. Lee, *Small*, 2014, **10**, 4106–12.

33 K. H. Bae, M. Park, M. J. Do, N. Lee, J. H. Ryu, G. W. Kim, C. Kim, T. G. Park and T. Hyeon, *ACS Nano*, 2012, **6**, 5266–73.

34 S. Laurent, S. Dutz, U. O. Häfeli and M. Mahmoudi, *Adv. Colloid Interface Sci.*, 2011, **166**, 8–23.

35 J. Xie, Y. Zhang, C. Yan, L. Song, S. Wen, F. Zang, G. Chen, Q. Ding, C. Yan and N. Gu, *Biomaterials*, 2014, **35**, 9126–36.

36 S. Ravi and A. Karthikeyan, *Phys. Procedia*, 2014, **54**, 45–54.

37 A. Sadhu and S. Bhattacharyya, *Chem. Mater.*, 2014, **26**, 1702–1710.

38 M. Kačenka, O. Kaman, Z. Jirák, M. Maryško, P. Žvátora, S. Vratislav and I. Lukeš, *J. Appl. Phys.*, 2014, **115**, 17B525.

39 S. Keshri, V. Kumar, P. Wiśniewski and A. S. Kamzin, *Phase Transitions*, 2014, **87**, 468–476.

40 A. Tovstolytkin, S. Solopan, V. Kalita, S. Ryabchenko and A. Belous, in *International Conference on Oxide Materials for Electronic Engineering - fabrication, properties and applications (OMEE-2014)*, IEEE, 2014, pp. 77–78.

41 M. S. Anwar, S. Kumar, F. Ahmed, G. W. Kim and B. H. Koo, *J. Nanosci. Nanotechnol.*, 2012, **12**, 5523–5526.

42 R. Epherre, E. Duguet, S. Mornet, E. Pollert, S. Louguet, S. Lecommandoux, C. Schatz and G. Goglio, *J. Mater. Chem.*, 2011, **21**, 4393.

43 K. P. Shinde, N. D. Thorat, S. S. Pawar and S. H. Pawar, *Mater. Chem. Phys.*, 2012, **134**, 881–885.

44 Z. F. Zi, Y. P. Sun, X. B. Zhu, Z. R. Yang, J. M. Dai and W. H. Song, *J. Magn. Magn. Mater.*, 2009, **321**, 2378–2381.

45 D. R. Sahu, B. K. Roul, P. Pramanik and J.-L. Huang, *Phys. B Condens. Matter*, 2005, **369**, 209–214.

46 A. Rostamnejadi, H. Salamati, P. Kameli and H. Ahmadvand, *J. Magn. Magn. Mater.*, 2009, **321**, 3126–3131.

47 V. Ravi, S. D. Kulkarni, V. Samuel, S. N. Kale, J. Mona, R. Rajgopal, A. Daundkar, P. S. Lahoti and R. S. Joshee, *Ceram. Int.*, 2007, **33**, 1129–1132.

48 N. D. Thorat, K. P. Shinde, S. H. Pawar, K. C. Barick, C. A. Betty and R. S. Ningthoujam, *Dalton Trans.*, 2012, **41**, 3060–71.

49 C. Sun, J. S. H. Lee and M. Zhang, *Adv. Drug Deliv. Rev.*, 2008, **60**, 1252–65.

50 J. Xie, G. Liu, H. S. Eden, H. Ai and X. Chen, *Acc. Chem. Res.*, 2011, **44**, 883–92.

51 C. Xu and S. Sun, *Adv. Drug Deliv. Rev.*, 2013, **65**, 732–43.

52 A. Verma and F. Stellacci, *Small*, 2010, **6**, 12–21.

53 K. R. Bhayani, S. N. Kale, S. Arora, R. Rajagopal, H. Mamgain, R. Kaul-Ghanekar, D. C. Kundaliya, S. D. Kulkarni, R. Pasricha, S. D. Dhole, S. B. Ogale and K. M. Paknikar, *Nanotechnology*, 2007, **18**, 345101.

54 N. D. Thorat, V. M. Khot, A. B. Salunkhe, R. S. Ningthoujam and S. H. Pawar, *Colloids Surf. B. Biointerfaces*, 2013, **104**, 40–7.

55 N. D. Thorat, S. V Otari, R. M. Patil, R. A. Bohara, H. M. Yadav, V. B. Koli, A. K. Chaurasia and R. S. Ningthoujam, *Dalton Trans.*, 2014, **43**, 17343–51.

56 N. D. Thorat, V. M. Khot, A. B. Salunkhe, A. I. Prasad, R. S. Ningthoujam and S. H. Pawar, *J. Phys. D. Appl. Phys.*, 2013, **46**, 105003.

57 N. D. Thorat, S. V Otari, R. A. Bohara, H. M. Yadav, V. M. Khot, A. B. Salunkhe, M. R. Phadatare, A. I. Prasad, R. S. Ningthoujam and S. H. Pawar, *Mater. Sci. Eng. C. Mater. Biol. Appl.*, 2014, **42**, 637–46.

58 N. D. Thorat, R. M. Patil, V. M. Khot, A. B. Salunkhe, A. I. Prasad, K. C. Barick, R. S. Ningthoujam and S. H. Pawar, *New J. Chem.*, 2013, **37**, 2733.

59 O. Pana, R. Turcu, M. L. Soran, C. Leostean, E. Gautron, C. Payen and O. Chauvet, *Synth. Met.*, 2010, **160**, 1692–1698.

60 R. Hergt, S. Dutz, R. Müller and M. Zeisberger, *J. Phys. Condens. Matter*, 2006, **18**, S2919–S2934.

61 S. Mornet, S. Vasseur, F. Grasset and E. Duguet, *J. Mater. Chem.*, 2004, **14**, 2161.

62 E. Natividad, M. Castro, G. Goglio, I. Andreu, R. Epherre, E. Duguet and A. Mediano, *Nanoscale*, 2012, **4**, 3954–62.

63 S. Manzoor, A. Ahmed, A. ur Rashid, S. N. Ahmad and S. A. Shaheen, *IEEE Trans. Magn.*, 2013, **49**, 3504–3507.

64 N. K. Prasad, K. Rathinasamy, D. Panda and D. Bahadur, *J. Biomed. Mater. Res. B. Appl. Biomater.*, 2008, **85**, 409–16.

65 R. Rajagopal, J. Mona, S. N. Kale, T. Bala, R. Pasricha, P. Poddar, M. Sastry, B. L. V. Prasad, D. C. Kundaliya and S. B. Ogale, *Appl. Phys. Lett.*, 2006, **89**, 023107.

66 O. Kaman, E. Pollert, P. Veverka, M. Veverka, E. Hadová, K. Knízek, M. Marysko, P. Kaspar, M. Klementová, V. Grünwaldová, S. Vasseur, R. Epherre, S. Mornet, G. Goglio and E. Duguet, *Nanotechnology*, 2009, **20**, 275610.

67 R. Rajagopal, J. Mona, S. N. Kale, T. Bala, R. Pasricha, P. Poddar, M. Sastry, B. L. V. Prasad, D. C. Kundaliya and S. B. Ogale, *Appl. Phys. Lett.*, 2006, **89**, 023107.

68 N. Singh, G. J. S. Jenkins, R. Asadi and S. H. Doak, *Nano Rev.*, 2010, **1**.

69 S. N. Kale, S. Arora, K. R. Bhayani, K. M. Paknikar, M. Jani, U. V Wagh, S. D. Kulkarni and S. B. Ogale, *Nanomedicine*, 2006, **2**, 217–21.

70 S. Daengsakul, C. Mongkolkachit, C. Thomas, S. Siri, I. Thomas, V. Amornkitbamrung and S. Maensiri, *Appl. Phys. A*, 2009, **96**, 691–699.

71 J. Overgaard, *Int. J. Radiat. Oncol.*, 1980, **6**, 1507–1517.

72 K. R. Kase and G. M. Hahn, *Eur. J. Cancer*, 1976, **12**, 481–491.

73 E. P. Armour, D. McEachern, Z. Wang, P. M. Corry and A. Martinez, *Cancer Res.*, 1993, **53**, 2740–2744.

74 Y. Nishimura, M. Hiraoka, S. Jo, K. Akuta, Y. Yukawa, Y. Shibamoto, M. Takahashi and M. Abe, *Int. J. Radiat. Oncol.*, 1988, **15**, 411–420.

75 L. F. Fajardo, S. D. Prionas, J. Kowalski and H. H. Kwan, 2010.

76 B. Gungor, I. Gombos, T. Crul, F. Ayaydin, L. Szabó, Z. Török, L. Mátés, L. Vígh and I. Horváth, *PLoS One*, 2014, **9**, e89136.

77 A. Pawlik, J. M. Nowak, D. Grzanka, L. Gackowska, J. Michalkiewicz and A. Grzanka, *Acta Histochem.*, 2013, **115**, 8–15.

78 P. Remani, V. V Ostapenko, K. Akagi, V. . Bhattathiri, M. Krishnan Nair and Y. Tanaka, *Cancer Lett.*, 1999, **144**, 117–123.

79 L. Wang, J. Dong, W. Ouyang, X. Wang and J. Tang, *Oncol. Rep.*, 2012, **27**, 719–26.

80 C. Theriault, E. Paetzell, R. Chandrasekar, C. Barkey, Y. Oni and W. O. Soboyejo, *Mater. Sci. Eng. C*, 2012, **32**, 2242–2249.

81 I. Belhadj Slimen, T. Najar, A. Ghram, H. Dabbebi, M. Ben Mrad and M. Abdrabbah, *Int. J. Hyperthermia*, 2014, **30**, 513–23.

82 B. Hildebrandt, *Crit. Rev. Oncol. Hematol.*, 2002, **43**, 33–56.

83 K. R. Bhayani, J. M. Rajwade and K. M. Paknikar, *Nanotechnology*, 2013, **24**, 015102.

84 K. F. Chu and D. E. Dupuy, *Nat. Rev. Cancer*, 2014, **14**, 199–208.

85 J. F. R. Kerr, C. M. Winterford and B. V. Harmon, *Cancer*, 1994, **73**, 2013–2026.

86 A. Sen, M. L. Capitano, J. A. Spernyak, J. T. Schueckler, S. Thomas, A. K. Singh, S. S. Evans, B. L. Hylander and E. A. Repasky, *Cancer Res.*, 2011, **71**, 3872–80.

87 C. W. Song, A. Lokshina, J. G. Rhee, M. Patten and S. H. Levitt, *IEEE Trans. Biomed. Eng.*, 1984, **31**, 9–16.

88 M. Babincov, V. Altanerov, C. Altaner, C. Bergemann and P. Babinec, *IEEE Trans. Nanobioscience*, 2008, **7**, 15–9.

89 G. A. Koning, A. M. M. Eggermont, L. H. Lindner and T. L. M. ten Hagen, *Pharm. Res.*, 2010, **27**, 1750–4.

90 Y. Mi, X. Liu, J. Zhao, J. Ding and S.-S. Feng, *Biomaterials*, 2012, **33**, 7519–29.

91 S. Singh, A. Armstrong, J. Robke, S. Waggoner and R. Debernardo, *Gynecol. Oncol. Case Reports*, 2014, **9**, 24–25.

92 J. Sun, Y. Song, Z. Wang, P. Gao, X. Chen, Y. Xu, J. Liang and H. Xu, *BMC Cancer*, 2012, **12**, 526.

93 S. Mulier, J.-P. Claes, V. Dierieck, J.-O. Amiel, J.-P. Pahaut, L. Marcelis, F. Bastin, D. Vanderbeeken, C. Finet, S. Cran and T. Velu, *Curr. Pharm. Des.*, 2012, **18**, 3793–3803.

94 A. M. Westermann, E. L. Jones, B.-C. Schem, E. M. van der Steen-Banasik, P. Koper, O. Mella, A. L. J. Uitterhoeve, R. de Wit, J. van der Velden, C. Burger, C. L. van der Wilt, O. Dahl, L. R. Prosnitz and J. van der Zee, *Cancer*, 2005, **104**, 763–70.

95 S. T. Heijkoop, M. Franckena, M. G. J. Thomeer, I. A. Boere, C. Van Montfort and H. C. Van Doorn, 2012.

96 M. Franckena, *Int. J. Hyperthermia*, 2012, **28**, 543–8.

97 M. D. Hurwitz, J. L. Hansen, S. Prokopios-Davos, J. Manola, Q. Wang, B. A. Bornstein, K. Hynynen and I. D. Kaplan, *Cancer*, 2011, **117**, 510–6.

98 K. Maier-Hauff, R. Rothe, R. Scholz, U. Gneveckow, P. Wust, B. Thiesen, A. Feussner, A. von Deimling, N. Waldoefner, R. Felix and A. Jordan, *J. Neurooncol.*, 2007, **81**, 53–60.

99 Q. Xiao, X. Zheng, W. Bu, W. Ge, S. Zhang, F. Chen, H. Xing, Q. Ren, W. Fan, K. Zhao, Y. Hua and J. Shi, *J. Am. Chem. Soc.*, 2013, **135**, 13041–13048.

100 F. S. Carvalho, A. Burgeiro, R. Garcia, A. J. Moreno, R. A. Carvalho and P. J. Oliveira, *Med. Res. Rev.*, 2014, **34**, 106–35.

101 F. Tulubas, A. Gurel, M. Oran, B. Topcu, V. Caglar and E. Uygur, *Toxicol. Ind. Health*, 2013, 0748233713483203–.

102 V. Fodale, M. Pierobon, L. Liotta and E. Petricoin, *Cancer J.*, **17**, 89–95.

103 S. Louguet, B. Rousseau, R. Epherre, N. Guidolin, G. Goglio, S. Mornet, E. Duguet, S. Lecommandoux and C. Schatz, *Polym. Chem.*, 2012, **3**, 1408.

104 M. Gogoi, H. D. Sarma, D. Bahadur and R. Banerjee, *Nanomedicine (Lond).*, 2014, **9**, 955–70.

105 M. Kačenka, O. Kaman, J. Kotek, L. Falteisek, J. Černý, D. Jirák, V. Herynek, K. Zacharovová, Z. Berková, P. Jendelová, J. Kupčík, E. Pollert, P. Veverka and I. Lukeš, *J. Mater. Chem.*, 2011, **21**, 157.

106 Z. Berkova, D. Jirak, K. Zacharovova, I. Lukes, Z. Kotkova, J. Kotek, M. Kacenka, O. Kaman, I. Rehor, M. Hajek and F. Saudek, *ChemMedChem*, 2013, **8**, 614–21.

107 R. Haghniaz, K. R. Bhayani, R. D. Umrani and K. M. Paknikar, *RSC Adv.*, 2013, **3**, 18489.

108 A. Giri, A. Makhal, B. Ghosh, A. K. Raychaudhuri and S. K. Pal, *Nanoscale*, 2010, **2**, 2704–9.

109 M. Kačenka, O. Kaman, S. Kikerlová, B. Pavlů, Z. Jirák, D. Jirák, V. Herynek, J. Černý, F. Chaput, S. Laurent and I. Lukeš, *J. Colloid Interface Sci.*, 2015, **447**, 97–106.

110 Z. Berkova, D. Jirak, K. Zacharovova, I. Lukes, Z. Kotkova, J. Kotek, M. Kacenka, O. Kaman, I. Rehor, M. Hajek and F. Saudek, *ChemMedChem*, 2013, **8**, 614–21.

111 S. V. Jadhav, D. S. Nikam, V. M. Khot, N. D. Thorat, M. R. Phadatare, R. S. Ningthoujam, A. B. Salunkhe and S. H. Pawar, *New J. Chem.*, 2013, **37**, 3121.

112 S. V. Jadhav, D. S. Nikam, V. M. Khot, S. S. Mali and S. H. Pawar, *Mater. Charact.*, 2015, **102**, 209–220.

113 D. H. Manh, P. T. Phong, P. H. Nam, D. K. Tung, N. X. Phuc and I.-J. Lee, *Phys. B Condens. Matter*, 2014, **444**, 94–102.

114 P. B. Shete, R. M. Patil, N. D. Thorat, A. Prasad, R. S. Ningthoujam, S. J. Ghosh and S. H. Pawar, *Appl. Surf. Sci.*, 2014, **288**, 149–157.

115 R. Haghniaz, R. D. Umrani and K. M. Paknikar, *Int. J. Nanomedicine*, 2015, **10**, 1609–23.

116 P. Veverka, O. Kaman, M. Kačenka, V. Herynek, M. Veverka, E. Šantavá, I. Lukeš and Z. Jirák, *J. Nanoparticle Res.*, 2015, **17**, 33.

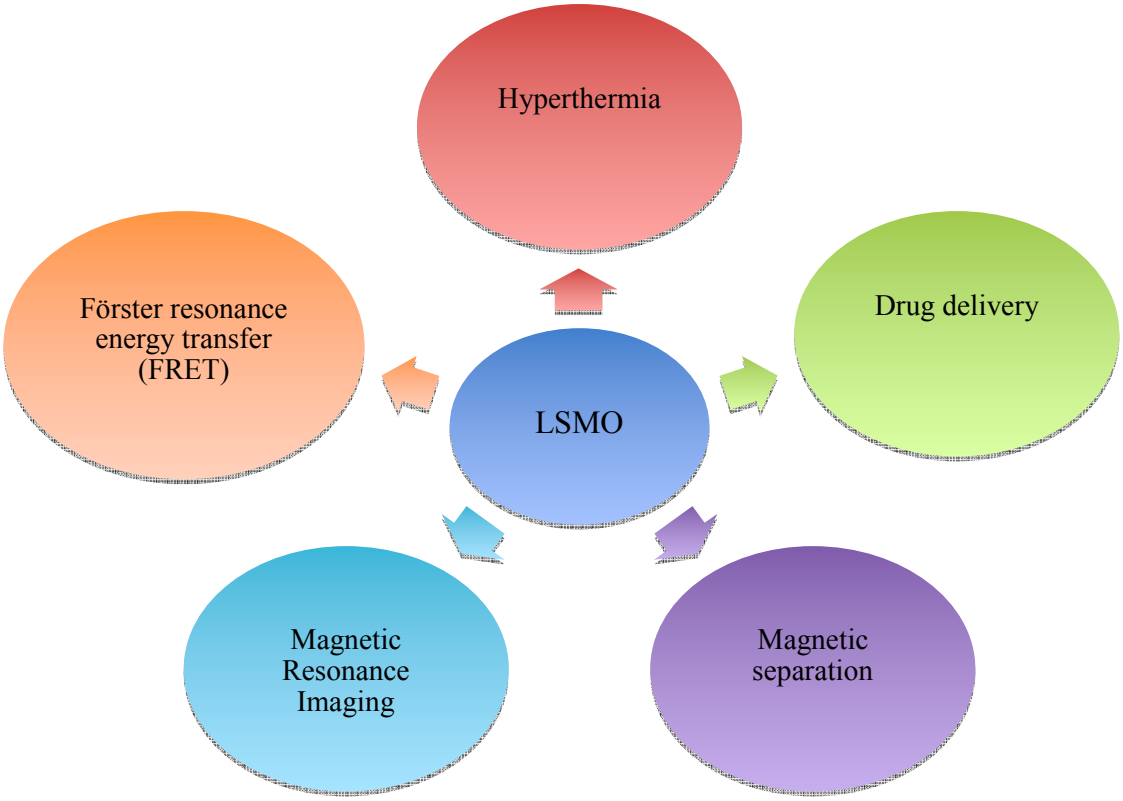

Multiple uses of LSMO nanoparticles in anticancer therapy.